15

Infrared Analysis of Electrostatic Layer-By-Layer Polymer Membranes Having Characteristics of Heavy Metal Ion Desalination

Weimin Zhou, Huitan Fu and Takaomi Kobayashi*
Department of Materials Science and Technology,
Nagaoka University of Technology, Kamitomioka, Nagaoka
Japan

1. Introduction

Layer-by-layer (LbL) self-assembly is a spontaneous and reversible organization process of interacting organic and polymeric components by their aggregation into ordered structures on substrate. LbL self-assembly process which occurs due to sequential adsorption of materials with complementary functional groups. Producing robust films and allow a precise control over the film thickness and its properties. This technique has been widely applied for the fabrication of multilayer films of organic and polymeric compounds, organic-inorganic hybrid structures, larger objects such as latex particles, and even purely inorganic thin films. By combining various functional materials for the formation of self-assembly multilayer, the LbL technique has led to a wide range of novel materials for various applications.[1,2]

It has been noticed that the LbL fabrication is usually guided by a driving force of hydrophobic interaction,[3] hydrogen-bond,[4] covalent bonding[5] and electrostatic interaction[6] between assembled compounds. Among those driving forces, electrostatic interaction between oppositely charged molecules becomes a very fascinating and attractive approach because of its simplicity and efficiency. The technique of alternate layer-by-layer assembly of cationic and anionic polyelectrolytes, generally referred to electrostatic self-assembly (ESA) as a firstly reported by Decher et al in 1991.[7] They took advantage of the charge-charge interaction between oppositely charged layers to create electrolytes multilayer. The polyelectrolyte conformation and layer interpenetration were due to an idealization of the surface charge reversal with each adsorption step which was based on the electrostatically driven multilayer build-up depicted.

ESA technique provided effective surface modification for thin film and separation membrane.[8, 9]Because the substrate surface contained negatively or positively charged due to the alternate deposition of polycation or polyanion, the transmission of charged particles like ions through self-assembly polyelectrolyte multilayer membrane might be affected by the charged surface. It was also showed that the presence of fixed charges at the surface of the multilayer resulted in Donnan exclusion of multivalent ions as well as the preferential transport of small

* Corresponding Author

monovalent ions.[8] Selective ion transport behaviour through ESA composite multilayer films was studied by Take[8] and Schelenoff.[9] The results suggested that highly specific ion separation was achieved and was affected by the charge and size of ion that pass through the composite multilayer. These researches made the polyelectrolytes multilayers interesting for the application of water desalination like heavy metal ion removal.

Generally, in LbL systems, infrared analysis method is more important method in studying chemical structures [10, 11] of the membranes, because the membranes were usually formed with the hydrogen bond, ion interactions and others which were difficultly investigated using other fundamental analysis methods such as ^{1}H NMR, XRD (X-ray diffraction) and XPS (X-ray photoelectron spectroscopy). In such infrared (IR) analysis, for example, Arrondo et al. used the infrared (IR) spectroscopy to the study of membrane proteins because the assignment of IR protein bands in H_2O and in D_2O, one of the more difficult points in protein IR spectroscopy.[12] Similarly, reflection-infrared spectroscopy is a powerful technique for characterizing protein and peptide-membrane interactions.[13] Mauntele et. al., used the IR to analyze lipid–protein interaction. In his case, lipid protein interactions play a key role in the stability and function of various membrane proteins. The FT-IR technique was used for a label free analysis of the global secondary structural changes and local changes in the tyrosine microenvironment.[14]

Furthermore, the FT-IR analytical technique was applied in analysis of surface of membranes interacted with other materials. For instance, Luo et. al., fabricated the SPES/Nano-TiO_2 composite ultrafiltration membrane. In their studies, the TiO_2 nanoparticle self-assembly on the SPES membrane surface was confirmed by X-ray photoelectron spectroscopy (XPS) and FT-IR spectrometer. When the nano-TiO_2 was self-assembled on the SPES membrane the absorption peak at 1243 cm^{-1} attributes to the stretching vibration of the ether C-O-C bond in the SPES polymer shifted to 1239 cm^{-1}. The result of FT-IR spectrometer effectively verified the self-assembly process of nano-TiO_2 on the SPES membrane.[15]

In study of ionic exchange membrane, FT-IR method was usually used to analyze the chemical structures of formed membrane. Fang et. al., prepared novel anion exchange membranes based on the copolymer of methyl methacrylate, vinylbenzyl chloride and ethyl acrylate. The structure of membrane was mainly verified by measurement of FT-IR. This study remarkably showed the importance of FT-IR method in analysis of chemical structure of membranes.[16]

Ding et al., confirmed the thermal treatment of precursor composite poly(amic acid) tertiary amine salts (PAAS) membrane using FT-IR/ATR analysis at 150 °C, and obtained composite polyimide hollow fiber membranes. In their studies, the FT-IR spectroscopy effectively evaluated the imidization of the coating layer.[17]

These reports indicated that importance of IR spectroscopy in analysis of chemical structures of membranes and interactions of membranes with other materials. Accordingly, IR analysis could provide to verify the chemical structure of ESA membranes.

In this chapter, we introduce the ESA modified membranes by forming electrostatic alternate layers of cetyl trimethyl ammonium chloride (CTAC) and poly(acrylic acid) (PAA) onto charged copolyacrylonitrile membranes (Scheme 1). Along with surface characterization of the ESA multilayer, infrared analysis was carried out. Finally, we evaluated the adsorptive properties of ESA multilayer for Fe^{3+} and Fe^{2+}, and ESA membranes with chitosan microspheres / PAA for removing of Cu^{2+}.

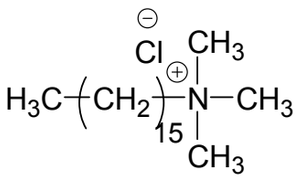

CTAC

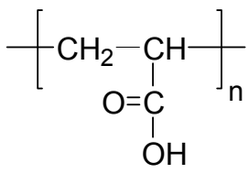

PAA

Scheme 1. Chemical structures of CTAC and PAA.

2. Multilayer composite surfaces prepared by an electrostatic self-assembly of quaternary ammonium salt or tetramethyl ammonium chloride and polyacrylic acid onto poly (acrylonitrile-*co*-acrylic acid) membrane

Preparation of composite multilayer on base membrane surface

Aqueous solutions with 1g / L concentration of CTAC, tetramethyl ammonium chloride (TMAC) and PAA were prepared respectively and used as dipping solutions for the surface modification of base P(AN-*co*-AA) membrane. As shown in Scheme 2-1, the preparation procedure consisted of the following four steps:

a. Immerging the base membrane into the CTAC or TMAC solution.
b. Washing away the loosely adsorbed cations by pure water.
c. Immerging into the PAA solution.
d. Washing out the excessive PAA anion adsorbed on membrane surface by pure water.

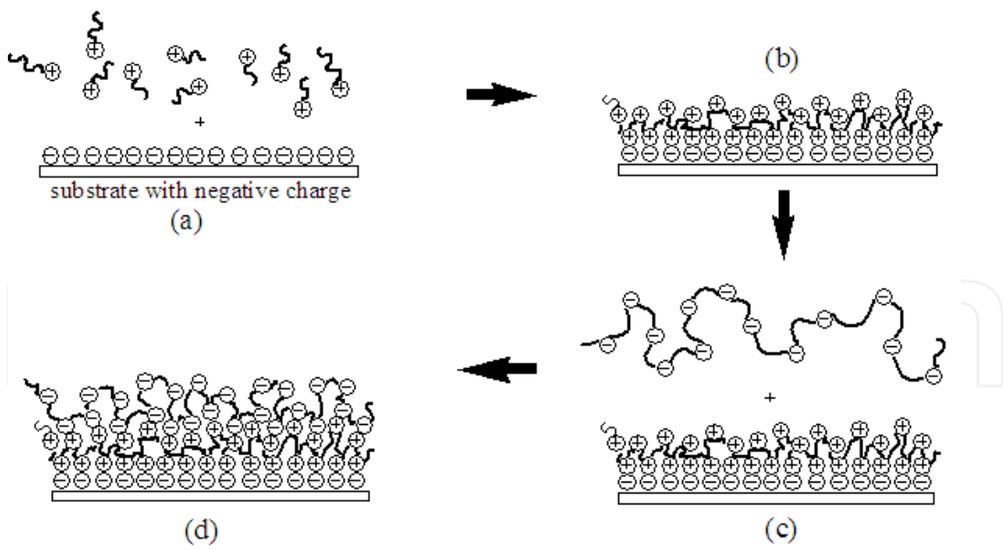

Scheme 2-1. Preparation procedure of ESA multi-layer on polymer membrane having negative charge.

By alternately immerging the base P(AN-*co*-AA) membrane into anion and cation solution as indicated by the four steps, ESA multiple layers of CTAC or TMAC and PAA could be formed on the negatively charged base membrane surface.

Confirmation of composite multilayer

The surface nature of resultant membranes modified with CTAC/PAA and TMAC/PAA ESA multiple layers would change alternately due to the alternate deposition of CTAC or TMAC and PAA layer on the surface. In order to estimate the formation of CTAC (or TMAC) and PAA layers on P(AN-*co*-AA) base membrane, the increment of membrane weight due to the repeated construction of composite layer on membrane surface was measured. Herein, we listed the weight value for each deposited layer of CTAC, TMAC and PAA. Here, the value of [DL] (Deposited Layer)(mmol / g) was calculated from [DL] = Δm / Fw, where Δm was the corresponding weight increment of membrane induced by each deposition step and Fw were 319.5 g / mol, 109.5 g / mol and 72 g / mol for CTAC, TMAC and PAA, respectively. The obtained average value of [DL] was about 1.4 mmol / g for P(AN-*co*-AA)/CTAC/PAA system and 1.6 mmol / g for P(AN-*co*-AA)/TMAC/PAA system.

FT-IR spectroscopy was applied to investigate the chemical component of resultant membranes as to confirm the formation of alternate layers of anion and cation. Figure 2-1 shows IR spectra of base P(AN-*co*-AA) and P(AN-*co*-AA) membranes for LbL of the CTAC/PAA composite multilayer on the surface. Spectrum (0) was for P(AN-*co*-AA), (1) for P(AN-*co*-AA) with CTAC monolayer, (2) for P(AN-*co*-AA)/CTAC/PAA, (3) for P(AN-*co*-AA)/CTAC/PAA/CTAC and (4) for P(AN-*co*-AA)/CTAC/PAA/CTAC/PAA. In the spectrum (0), there was a wide and strong absorption peak appeared near 3500-2800cm^{-1}, which was assigned to the dimmer formed by hydrogen bonds of carboxylic acids of the AA segments in the P(AN-*co*-AA). Also, the characteristic absorption peak assigned to

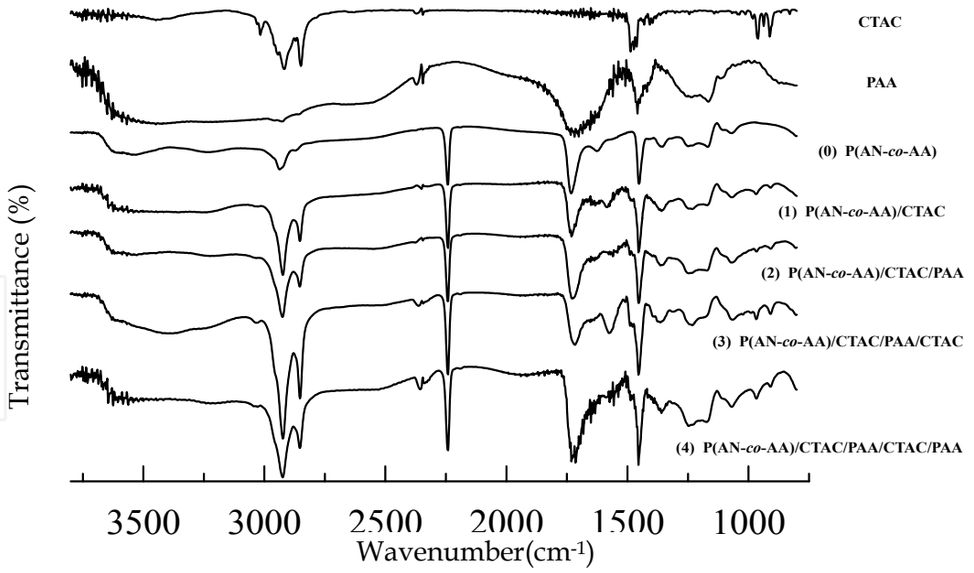

Fig. 2-1. Comparison of FT-IR spectra of the base P(AN-co-AA) and multi-layer composites of CTAC/PAA on the base P(AN-co-AA). The layer number of each spectrum was represented as 0, 1, 2, 3 and 4 for P(AN-co-AA), P(AN-co-AA)/CTAC, P(AN-co-AA)/CTAC/PAA, P(AN-co-AA)/CTAC/PAA/CTAC and P(AN-co-AA)/CTAC/PAA/CTAC/PAA, respectively.

dissociated carboxylic group at about 1645 cm^{-1} and 1720 cm^{-1} existed in the spectrum. In the spectrum (1), it was noticed that the absorption peak around 3500-2800 cm^{-1} became weaker, indicating that the dimmer band formed by hydrogen bonds was reduced due to the deposition of CTAC over membrane surface. Opposite to the increase of the C-H absorption strength at about 1454cm^{-1}, the C=O absorption strength at about 1737 cm^{-1} was somewhat lower than that of -C≡N band strength at 2300 cm^{-1}. From the obvious change of the membrane spectra after the deposition of CTAC layer, it was reasonable to say that the change of the chemical structure of LbL suggested the presence of part of carboxylic groups dissociated to react with CTAC by electrostatic attraction.

Compared to the amphiphilic CTAC, TMAC behaved similar cationic property except for long alkyl chain on the quaternary ammonium site. The FT-IR spectra of the base P(AN-*co*-AA), P(AN-*co*-AA) with TMAC monolayer and with TMAC/PAA composite multilayer are shown in Figure 2-2. Apparently, the dimmer band in the range from 3500-2800 cm^{-1} changed alternately after the formation of TMAC layer on the P(AN-*co*-AA) base membrane surface and then the PAA layer over the P(AN-*co*-AA)/TMAC. Also, the ratio of >C=O group at about 1720 cm^{-1} to that of the dissociated carboxylic group at about 1645 cm^{-1}

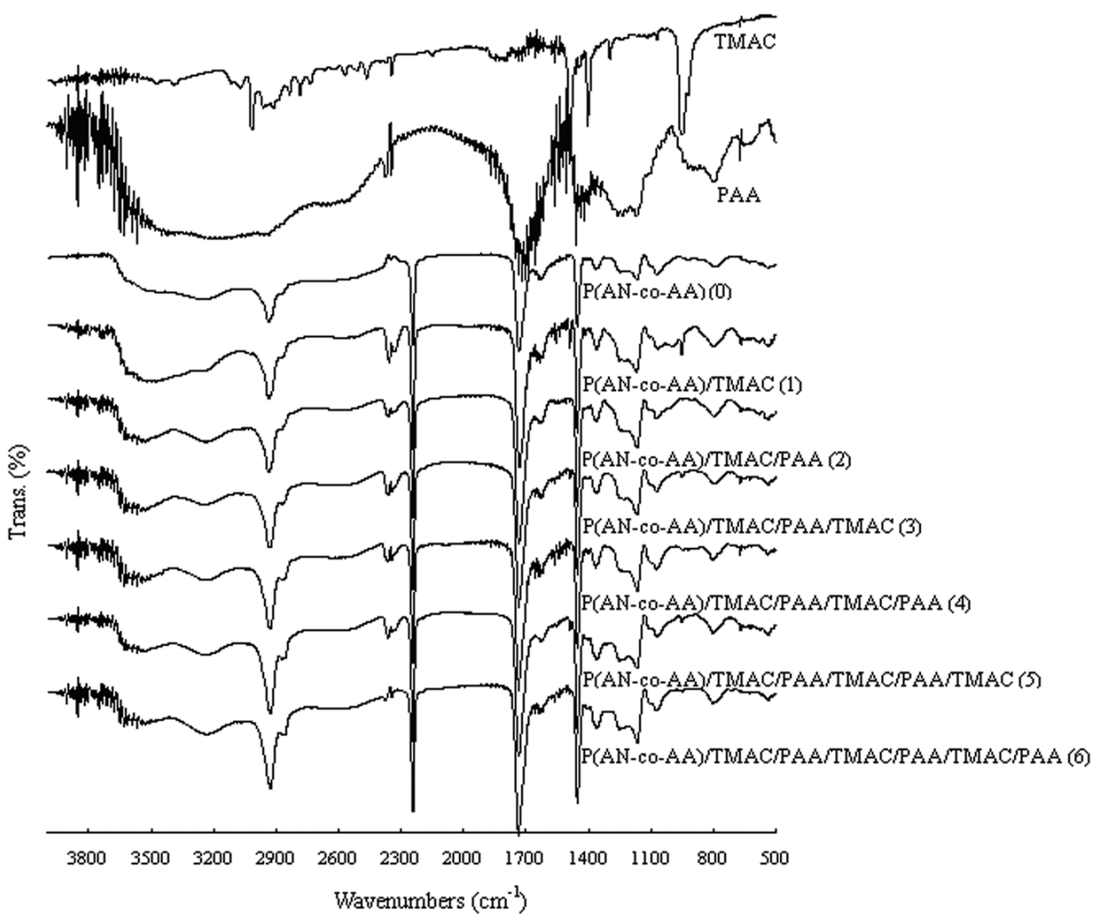

Fig. 2-2. Comparison of FT-IR spectra of the base P(AN-co-AA), P(AN-co-AA)/TMAC/PAA multi- layer composites, the layer numbers.

increased as the TMAC and PAA were deposited. The reason for this phenomena was same with the P(AN-*co*-AA)/CTAC/PAA system as induced by the fact that the deposition of TMAC layer over PAA layer enhanced the dissociation of carboxylic group which neutralized with TMAC molecules. FT-IR data also showed that the C-H absorption peak around 2920 cm^{-1} increased slightly as the number of TMAC layer increased. Moreover, characteristic absorption peak from TMAC at around 950 cm^{-1} appeared in the spectra of the resultant P(AN-*co*-AA) membrane with TMAC/PAA composites multilayer on the surface. Moreover, it was noticed that the strength of C-H absorption peak at 1454 cm^{-1} increased with the increase of composite layers on membrane surface, even through the changes were smaller as compared with P(AN-*co*-AA)/CTAC/PAA. All these changes confirmed the alternate construction of TMAC and PAA layers on base membrane surface which was induced by the electrostatic interaction between two neighboring layers.

Due to the electrostatic interaction between CTAC (or TMAC) and AA segments in the P(AN-*co*-AA) base membrane as well as between neighboring CTAC (or TMAC) and PAA layers, the composite multilayer of CTAC/PAA and TMAC/PAA successfully self-assembled. To reveal the alternate formation of self-assembly CTAC/PAA and TMAC/PAA multilayer qualitatively, the strength ratio of >C=O band at about 1737 cm^{-1} to 1654 cm^{-1} as shown in Figure 2-3 was calculated from FT-IR spectra. It was observed that the bond intensity of >C=O group decreased after the deposition of CTAC (or TMAC) layer as part of carboxylic groups of AA segment electrostatically associated with CTAC (or TMAC) the CTAC (or TMAC) layer, and then increased as the PAA layer was formed to be the top layer for the composite multilayer. This alternate change tendency revealed the dissociation extent change of carboxylic acid groups in base membrane or in each PAA layer and strongly confirmed the sequent adsorption of CTAC (or TMAC) and PAA layer on the negatively charged P(AN-*co*-AA) base membrane surface.

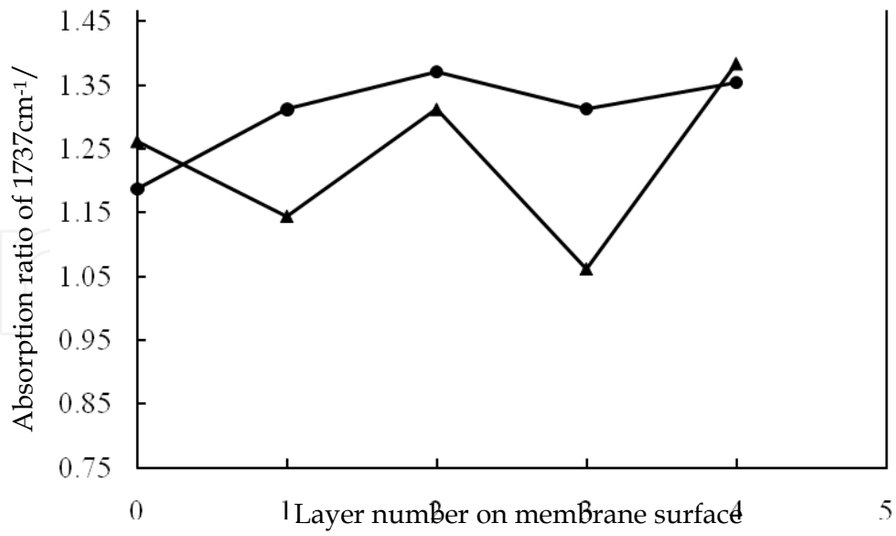

Fig. 2-3. Absorption ratio of observed IR bands for 1737cm^{-1}, 1645 cm^{-1} C=O assigned to carboxylic acid and to the dissociated carboxylic acid in IR spectra obtained in P(AN-co-AA)/CTAC/PAA (▲)and P(AN-co-AA)/TMAC/PAA (●) multilayer composites. The layer numbers were the same with those described in Figure 2-2.

3. Preparation of multilayer composite surfaces prepared by electrostatic self-assembled technique for desalination of Fe^{3+}, and Fe^{2+}

Multilayer desalination membranes

As presented in scheme 3-1, quaternized *N,N*-dimethylethyl ammonium bromide (EDAMA) was polymerized with AN for preparation of cationic base membrane. After that, AA and the quaternized EDAMA were used for their functional groups in order to provide charged sites for polyacrylonitrile base membranes. Also, Poly(acrylonitrile-*co*-acrylic acid) [P(AN-*co*-AA)] membrane was used as a negatively charged base, while Poly(acrylonitrile-*co*-*N,N*-dimethyethyl ammonium bromide P(AN-*co*-EDAMA) was used as a positively charged substrate.[18, 19]

Their base membranes of P(AN-*co*-AA) and P(AN-*co*-EDAMA) were prepared by phase-inversion of their respective dimethyl sulfoxide solutions in water.[20] The base membranes of P(AN-*co*-AA) or P(AN-*co*-EDAMA) were orderly dipped in positive CTAC and negative PAA aqueous solutions. After each deposition step, the resulting membranes were rinsed thoroughly with water. Such deposition process was repeated to obtain desired number of self-assembled layers. In this research, P(AN-*co*-AA) or P(AN-*co*-EDAMA) membranes with ESA layers are referred to as P(AN-*co*-AA)/CTAC/PAA system or as P(AN-*co*-EDAMA)/PAA/CTAC system, respectively.

Before measuring the properties of membranes with ESA multilayer, sample membranes were dehydrated using freeze-drying method in order to preserve the sample structure for the following characterization of the membrane properties.

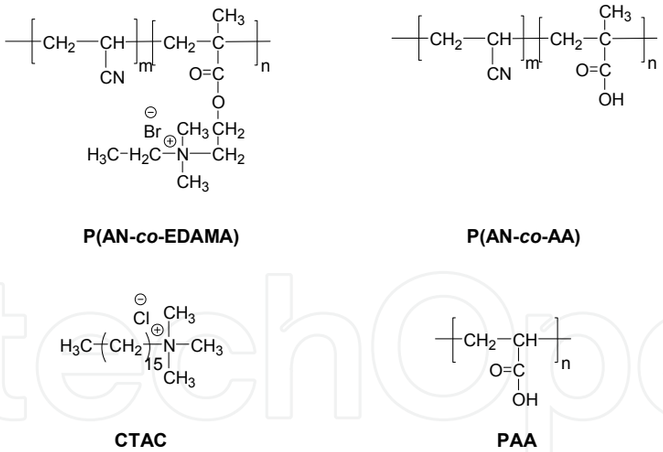

Scheme 3-1. Chemical structures of membrane materials P(AN-*co*-AA) and P(AA-*co*-EDAMA) and electrolytes of CTAC and PAA.

The metal-ion permselective properties were examined as follows: metal ion solutions containing $Fe(NO_3)_3$ and $FeCl_2$ with 2 ppm concentration were prepared, respectively. Before and after the formation of ESA layers, filtration measurement of the metal ion solution through sample membranes was carried out by using an ultrafiltration cell (Amicon 8010, 50 ml volume). The metal-ion rejection (R) was defined by the following equation:

$$R = (1 - c_t / c_o) \times 100\% \quad (3\text{-}1)$$

were C_o is the ionic concentration in the feed solution and C_t is the ionic concentration in the permeate solution after a time *t*.

In order to evaluate the selective rejection property of the resultant membranes, the removal selectivity coefficient (S_R) for Fe^{3+} and Fe^{2+} ions was calculated from the following equation:

$$S_R = R_{Fe^{3+}} / R_{Fe^{2+}} \quad (3\text{-}2)$$

$R_{Fe^{3+}}$ and $R_{Fe^{2+}}$ were the rejection values of the resultant membranes for Fe^{3+} and Fe^{2+}, respectively.

IR measurement of membranes with ESA multilayer

As presented in Scheme 3-2, the base membrane surface was modified alternately by layer-by-layer formation of CTAC and PAA via ESA treatment. The structure of membrane formed in P(AN-co-AA)/CTAC/PAA system is shown in Figure 2-1. In this section, we mainly introduced the analysis of structure of membrane formed in P(AN-*co*-EDAMA)/PAA/CTAC system. In Figure 3-1, the FT-IR spectrum indicated that for the positively charged substrate of P(AN-*co*-EDAMA), the ESA treatment was performed in the deposition cycle order of PAA/CTAC/PAA/CTAC. As a result of the first deposition of the PAA layer, the band strength of the carboxylic group at about 1720 cm^{-1} became stronger, which confirmed the assembly of the PAA layer onto the positively charged base membrane. However, after the deposition of CTAC layer, the carboxylic groups bound on the CTAC

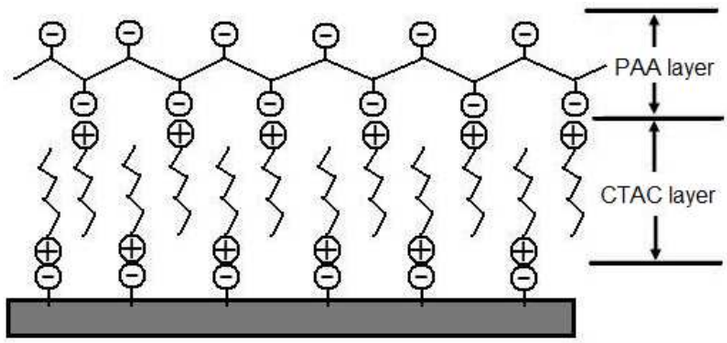

(a) P(AN-co-AA)/CTAC/PAA system

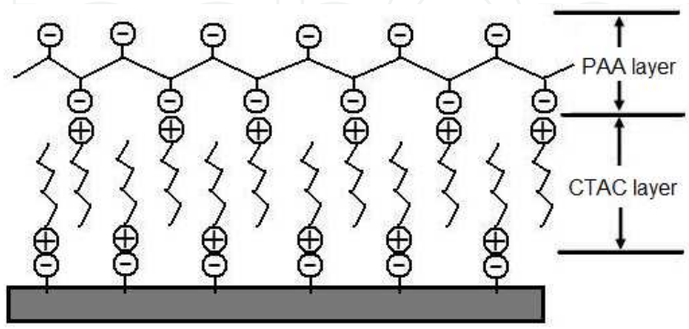

(b) P(AN-*co*-EDAMA)/PAA/CTAC system

Scheme 3-2. Illustration images of layer-by-layer assembling of CTAC and PAA on negatively charged P(AN-*co*-AA) membrane surface (a) and on positively charged P(AN-*co*-EDAMA) membrane surface (b).

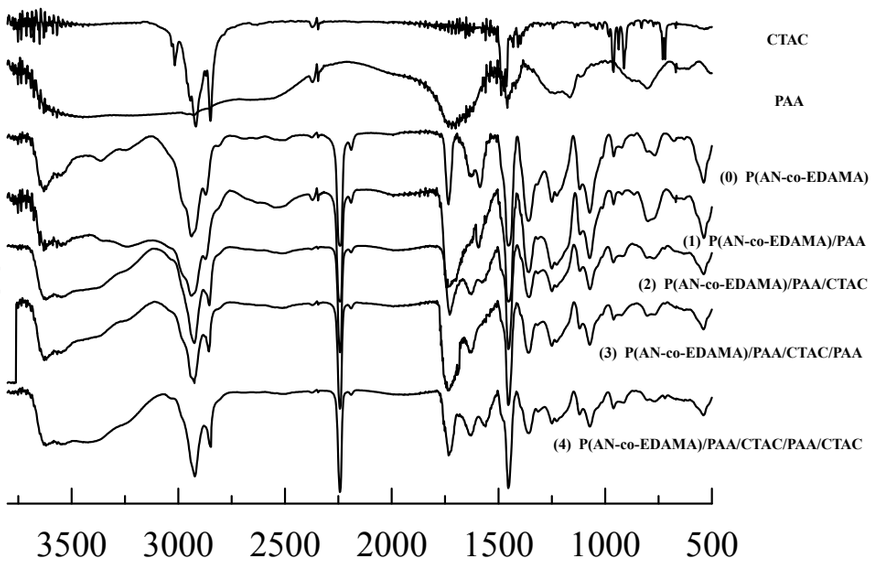

Fig. 3-1. FT-IR spectra of base membrane and membrane with self-assembled layers.

layer resulted that the carboxylic acid absorption peak became weaker relative to that of P(AN-*co*-EDAMA)/PAA. A similar tendency repeated itself in accordance with the self-assembly of the first cycle of PAA layer and CTAC layer. Hereby, the alternate self-assembly of CTAC and PAA onto the charged base membranes of P(AN-*co*-AA) and P(AN-*co*-EDAMA) was confirmed by the FT-IR measurement.

Since the alternate ESA layers on the membrane surface contained charged groups, it was expected that the permeate behaviour of metal ions through the modified membrane could be affected by the ESA layers formed on the membrane surface.[21, 22] Thus, the desalination of the ESA modified membranes was evaluated by testing the permeability for metal ion solution. Rejection values for metal ions of Fe^{3+} and Fe^{2+} of resultant membranes of the P(AN-*co*-AA)/CTAC/PAA system and P(AN-*co*-EDAMA)/PAA/CTAC system are shown in Figure 3-2 and Figure 3-3, respectively, with solid lines for Fe^{3+} and dotted lines for Fe^{2+}. It could be seen that the membrane modified with ESA layers showed considerable high rejection for metal ion of Fe^{3+} and the rejection for Fe^{3+} was higher than for Fe^{2+}. This may be induced by the smaller hydrated ion radius of Fe^{2+} than that of Fe^{3+} resulting from the fact that Fe^{2+} has a bigger ion radius of about 0.78 nm than the 0.64 nm of Fe^{3+}. As revealed by both of the two systems, the metal-ion rejection was strongly related to the charge property of the outer layer on the modified membrane surface. It was noted interestingly that the metal ion rejection changed alternately and was higher in deposition cycle of 1, 3 and 5 for the P(AN-*co*-AA)/CTAC/PAA system, while higher in deposition cycle of 2, 4 and 6 for the P(AN-*co*-EDAMA)/PAA/CTAC system. It seemed that the deposition of CTAC layers having positively charged groups enhanced the rejection of membranes for metal ions, might be due to the electrostatic repulsion between metal ion and the CTAC layer on membrane surface. Therefore, it was considered that membrane having the LbL surface terminated by positively charged species, due to the self-assembly of CTAC layers might be effective for the metal ion removal application.

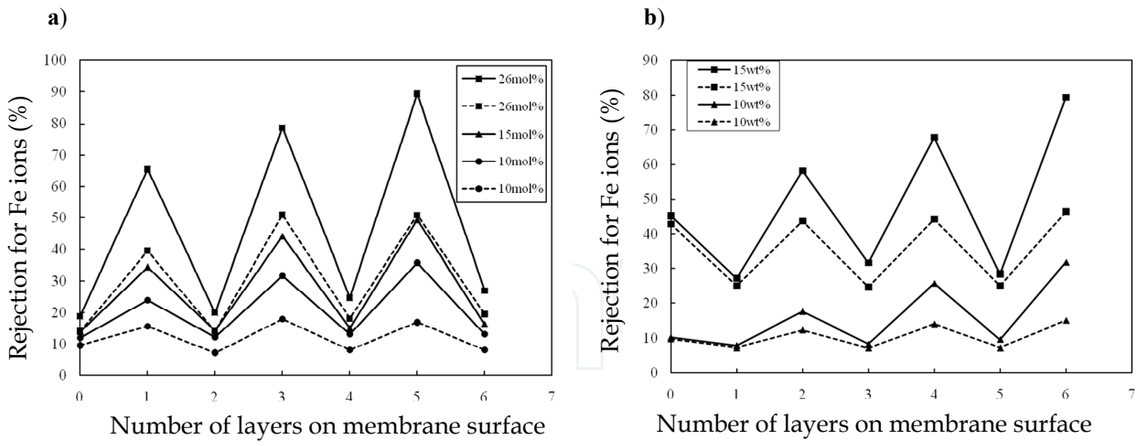

Fig. 3-2. **a**) The effect of AA fraction contained in base membrane on the rejection of Fe^{3+} (—) and Fe^{2+} (…) for P(AN-co-AA)/CTAC/PAA system (cast solution concentration for base membrane: 15wt%; pH of metal ions solution: 7). **b**) The effect of P(AN-*co*-EDAMA) base membrane on the rejection of Fe^{3+} (—) and Fe^{2+} (…) for P(AN-*co*-EDAMA)/PAA/CTAC system. (EDAMA contained in base membrane: 2 mol%; pH of metal ions solution: 7).

Additionally, the change tendency of the rejection curves of the two systems for both metal ions behaved oppositely to each other as revealed by Figure 3-2. These indicated that P(AN-*co*-AA) base membrane having COO^- on the surface was negatively charged, while P(AN-*co*-EDAMA) base membrane having quatemary ammonium groups on the surface was negatively charged. Their different charge properties of base membrane surface resulted in different cycle order of self-assembled multilayer deposited on the base membrane surface, as performed in cycle of CTAC/PAA/CTAC/PAA for the former and PAA/CTAC/PAA/CTAC for the latter. The opposite change tendency of the permeability of resultant membranes further confirmed the influence of the ESA terminal layer on its permeability.

Furthermore, we examined the effect of base membrane structure on the rejection behavior of resultant membrane. For P(AN-*co*-AA)/CTAC/PAA system, the charged sites on P(AN-*co*-AA) base membrane were different for membranes having different amounts of AA segments.

Three kinds of P(AN-*co*-AA) copolymers prepared with a AA fraction of 10 mol%, 15 mol% and 26 mol%,[23] were used as base membranes for ESA treatment. Then, the surfaces were modified with ESA layers of CTAC and PAA to study the effect of AA fractions contained in the base membrane on the removal properties of modified membranes. It was found that, when the base membrane used for self-assembly treatment contained higher AA mol%, the corresponding resultant membranes showed higher removal properties for both Fe^{3+} and Fe^{2+}. This meant that base membrane which contained higher AA mol% had more ionized carboxyl charged sites on the surface. Then, there would be more CTAC and PAA adsorbed onto membrane surface during the alternate dipping process, leading to resultant membrane surface having higher charge density and then affecting the permeability for metal ions. For the P(AN-*co*-EDAMA)/PAA/CTAC system, by increasing the concentration of the cast solution, the effect of the base membrane structure on the permeability of ESA layer modified membranes was studied. As shown in Figure 3-2(b), when the P(AN-*co*-EDAMA)

base membrane was prepared by cast solution with a higher concentration of 15%, the rejection for Fe^{3+} and Fe^{2+} rose significantly as compared with that of membranes prepared with a concentration of 10%. This result was also induced by the higher charge density of base membrane prepared with higher concentration which consequently affected the formation of ESA layers onto charged base membrane surface.

To study the charge density of PAA layer on membrane surface, we calculated the ratio of dissociated COO^- group and COOH group by referring to the characteristic peaks at 1446 cm^{-1} and 1710 cm^{-1}, respectively, revealed by FT-IR data in Figure 2-1 and Figure 3-1. For the P(AN-*co*-AA)/CTAC/PAA system, the value of [COO^-]/[COOH] was 72% for base membrane of P(AN-*co*-AA), after the surface was converted with CTAC layer, the value became to be 78% and then decreased to 47 % due to the assembly of PAA layer onto membrane surface. Then, the value changed to be 83% and 49% consequently as the second circle of CTAC/PAA layers was formed onto membrane surface.

As the rejection of the resultant membranes for Fe^{3+} and Fe^{2+} was obviously different, it was considered that the resultant membranes were showed permselectivity for Fe^{3+} and Fe^{2+}. Herein, the removal selectivity coefficient for Fe^{3+} and Fe^{2+} was calculated according to equation 3-2. The results are shown in Table 3 for the P(AN-*co*-AA)/CTAC/PAA system and the P(AN-*co*-EDAMA)/CTAC/PAA system. The results indicated that membrane modified with ESA layers of CTAC and PAA was capable of selectively removing Fe^{3+} and Fe^{2+} along with relatively high selective permeability. For the P(AN-*co*-AA)/CTAC/PAA system, as shown in Table 3-(a) and 3-(b), base membrane containing 10 mol% AA segment (denoted by a) resulted in ESA modified membrane having relative higher removal selectivity coefficients (S_R) for metal ion pair of Fe^{3+} and Fe^{2+} as compared with base membrane containing 26 mol% AA segment. The results revealed that lower fraction of AA segments in the base membrane led to resultant membrane with lower selective

Number of ESA layers	1	2	3	4	5	6
S_R for Fe^{3+}/Fe^{2+} of P(AN-*co*-AA) [a)]	1.54±0.02	1.68±0.04	1.75±0.07	1.61±0.03	2.10±0.06	1.62±0.03
S_R for Fe^{3+}/Fe^{2+} of P(AN-*co*-AA) [b)]	1.64±0.03	1.42±0.01	1.53±0.04	1.36±0.05	1.75±0.06	1.37±0.06
S_R for Fe^{3+}/Fe^{2+} of P(AN-*co*-EDAMA)[c)]	1.07±0.04	1.32±0.05	1.28±0.05	1.52±0.02	1.13±0.06	1.69±0.03
S_R for Fe^{3+}/Fe^{2+} of P(AN-*co*-EDAMA) [d)]	1.07±0.03	1.42±0.02	1.15±0.05	1.82±0.06	1.33±0.04	2.10±0.04

(a) 10 mol% and (b) 26 mol% of AA in the P(AN-*co*-AA)s were used.
(c) 10 mol% and (d) 15 mol% of EDAMA were used in the P(AN-*co*-EDAMA).

Table 3. Selective removel coefficient (S_R) for Fe^{3+} / Fe^{2+} of the P(AN-*co*-AA)/CTAC/PAA system and Fe^{3+}/Fe^{2+} of the P(AN-*co*-EDAMA)/PAA/CTAC system.

permeability for Fe^{3+} and Fe^{2+}. This may be because that much of the electrolytes self-assembled onto membrane surface, which was enhanced by the higher charge density resulting from the higher fraction of AA segments in the base membrane. So the permeability of membrane for metal ion solution was weakened and then led to lower permselectivity.

Also, the base membrane used for ESA treatment contained 10 mol% AA segment, S_Rs for metal ion pair of Fe^{3+} and Fe^{2+} of the modified membranes terminated with CTAC, CTAC/PAA/CTAC and CTAC/PAA/CTAC/PAA/CTAC ESA layers were 1.54±0.02, 1.75±0.07 and 2.10±0.06, respectively.

While the S_Rs of membranes deposited with CTAC/PAA, CTAC/PAA/CTAC/PAA, CTAC/PAA/CTAC/PAA/CTAC/PAA ESA layers were 1.68±0.04, 1.61±0.03 and 1.62±0.03, respectively. It was reasonable to conclude that the resultant membrane was endued with higher selective removal property for Fe^{3+} and Fe^{2+} when the surface was self-assembly terminated with positive CTAC layer.

For P(AN-*co*-EDAMA)/PAA/CTAC system, the S_Rs for Fe^{3+} and Fe^{2+} ions are shown in Table 3-(c) and (d). It can obviously seen that base membrane prepared by 15 mol% cast solution of P(AN-*co*-EDAMA)(denoted by c) resulted in ESA modified membranes with higher S_R as compared with base membrane prepared with 10 mol% cast solution (denoted by d). When the base membrane used for ESA treatment was prepared by 15wt% cast solution of P(AN-*co*-EDMA), S_Rs of the corresponding resultant membranes modified with PAA/CTAC, PAA/CTAC/PAA/CTAC and PAA/CTAC/PAA/CTAC and PAA/CTAC/PAA/CTAC/PAA/CTAC multilayer were 1.42±0.02, 1.82±0.06 and 2.10±0.04, respectively, while the S_Rs of membranes having CTAC/PAA, CTAC/PAA/CTAC/PAA, CTAC/PAA/CTAC/PAA/CTAC/PAA layers on the surface became 1.07±0.03, 1.15±0.05 and 1.33±0.04, respectively. These indicated that positively charged surface induced by the formation of self-assembly CTAC layers was capable of selectively removing Fe^{3+} and Fe^{2+} ions. From these results, it was found out that for the P(AN-*co*-AA)/CTAC/PAA system, showed higher selectivity but lower rejection for Fe^{3+} and Fe^{2+}. While for the P(AN-*co*-EDAMA)/PAA/CTAC system, showed considerable high rejection for Fe^{3+} about 90% as well as a relative high permselectivity for Fe^{3+} and Fe^{2+}. It was proposed that the membranes prepared in this experimental could be used for the selective desalination of solution containing Fe^{3+} and Fe^{2+}.

4. Self-assembly functionalized membranes with chitosan microsphere / Polyacrylic acid layers and their application for metal ion removal of Cu^{2+}

Modification of PAN to anionic charged base membrane for adsorption of Cu (II)

PAN membrane, which was used as the base membrane for ESA treatment, was prepared and then treated with 2M KOH solution for negatively charged PAN base membrane (Scheme 4-1)[19].

Adsorption of Cu(II)

The adsorption experiment for Cu(II) was performed using the static method and was carried out as follows. Immerging the sample membranes was carried out into $CuSO_4$ solution with a concentration of 2 ppm for 40 min at room temperature and then, the

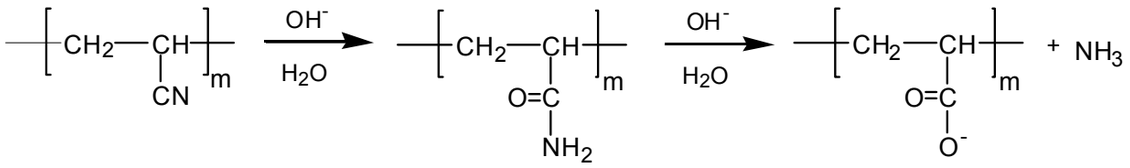

Scheme 4-1. Chemical reaction of PAN treated by alkali solution.

original and residual ion concentrations remained in the ion solution were measured by Atomic absorption spectrophotometer (AA-6300, Shimadzu Ins). The metal ion adsorption capacity (10^{-6} g / g-memebrane) was defined as the amount of Cu^{2+} (g) adsorbed by unit weight of membrane (g), and was calculated by following equation.

$$Cu(\text{II})(\textit{adsorption capacity}) = v(c_o\text{-}c_e)/M \quad (4\text{-}1)$$

where c_o is the initial concentration of Cu(II) (ppm/ml), C_e is the concentration at equilibrium, V is the volume (40 ml) of solution and M is the wet mass of resultant membrane being used.

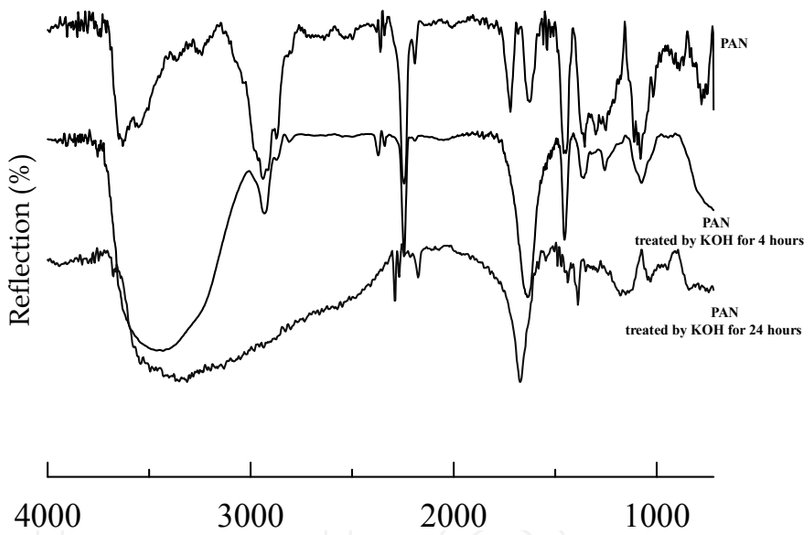

Fig. 4-1. FT-IR spectra of original PAN membrane and membrane treated with KOH solution.

In order to convent the CN groups to negatively charged COO^- group on the PAN membrane surface, the chemical reaction (Scheme 4-1) was performed by using KOH solution. The FT-IR measurement was carried out to study the chemical composition of the PAN membrane surface before and after the KOH treatment. In the spectrum of the PAN membrane treated by KOH for 24 hours, the characteristic absorption peak for the CN group at about 2300 cm^{-1} became weaker while the characteristic peak assigned to carboxyl group in the range from 2800 cm^{-1} to 3700 cm^{-1} appeared stronger. Especially, the band at 1700 cm^{-1} assigned to the carbonyl group from COO^- existed in the FT-IR spectrum. So, it was concluded that the PAN membrane surface was negatively charged due to the formation of carboxyl groups resulting from the KOH treatment.

Formation of the ESA multilayer of chitosan / PAA and chitosan microspheres / PAA

As the surface of treated PAN membrane was negatively charged due to the KOH treatment, positively charged chitosan and negatively charged PAA were alternatively coated to form self-assembly layers onto the charged PAN membrane (Scheme 4-2). Also, chitosan polycation microspheres cross-liked by sulfate groups were used instead of chitosan to form electrostatical self-assembled layers onto the negatively charged base membrane. The deposition process of the alternate formation of chitosan or chitosan microspheres and PAA layers was repeated 4 times. In Scheme 4-2, for the first step, the cationic chitosan or chitosan microspheres electrostatically interacted with the negatively charged groups on the base membrane surface. The membrane surface was then positively charged due to the deposition of chitosan or chitosan microspheres. Then, for the second step, PAA was deposited over the first layer of chitosan or chitosan microspheres due to the electrostatic interaction between amino groups of the chitosan and carboxyl groups of the PAA. These steps were repeated to form multiple ESA layers on the base membrane surface.

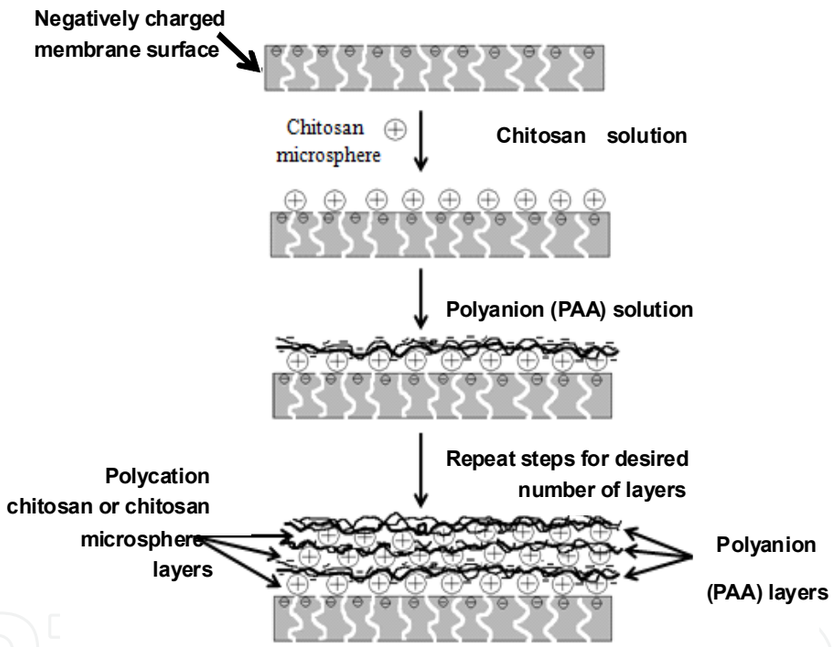

Scheme 4-2. Illustration images of layer-by-layer assembling of chitosan/PAA and chitosan microsphere/PAA layers onto charged base membrane.

In order to confirm the fabrication of the multilayer of chitosan or chitosan microsphere and PAA layers. Here, the FTIC labeled-chitosan and PAA layers were alternatively deposited onto charged glass slide for UV-vis measurement (Scheme 4-3).

The FTIC-labeled-chitosan (FTIC-labeled chitosan microsphere)/PAA layers on flat glass after each deposited cycle was detected by UV absorption at 476 nm. The UV absorption results of the samples were represented in Figure 4-2 and Figure 4-3, the odd layers were chitosan (chitosan microsphere) outmost. As we can see from Figure 4-2 that for both of PAN/chitosan/PAA system and PAN/chitosan microsphere/PAA system, the value of UV-absorption increased almost linearly with the increasing cycle of deposition process

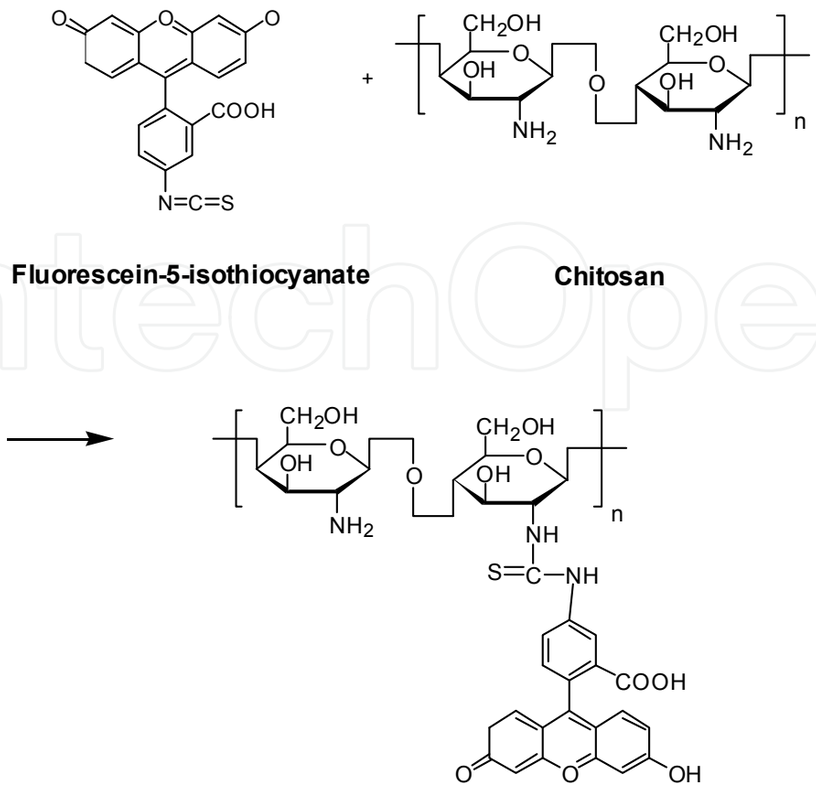

Scheme 4-3. Schematic illustration of the chemical synthesis of fluorescein isothiocyanate labelled (FITC) chitosan of free FTIC fluorescence signal in the washing medium.

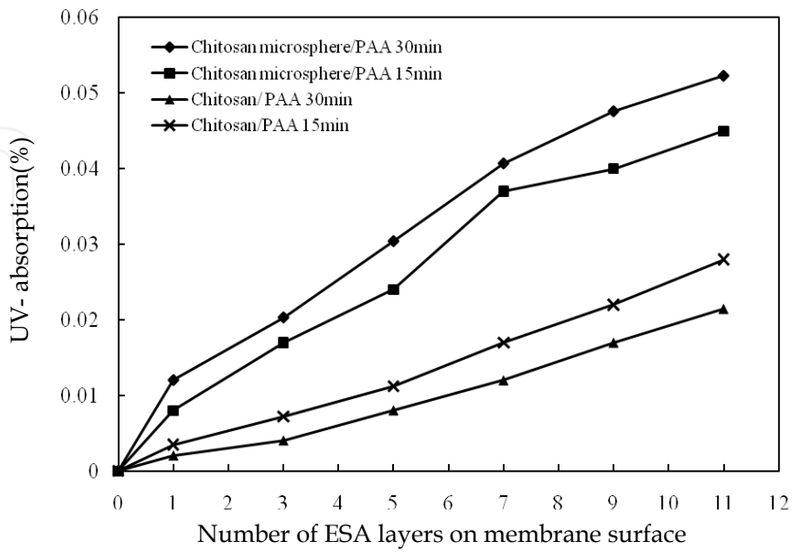

Fig. 4-2. UV-absorption after each deposition of chitosan layer.

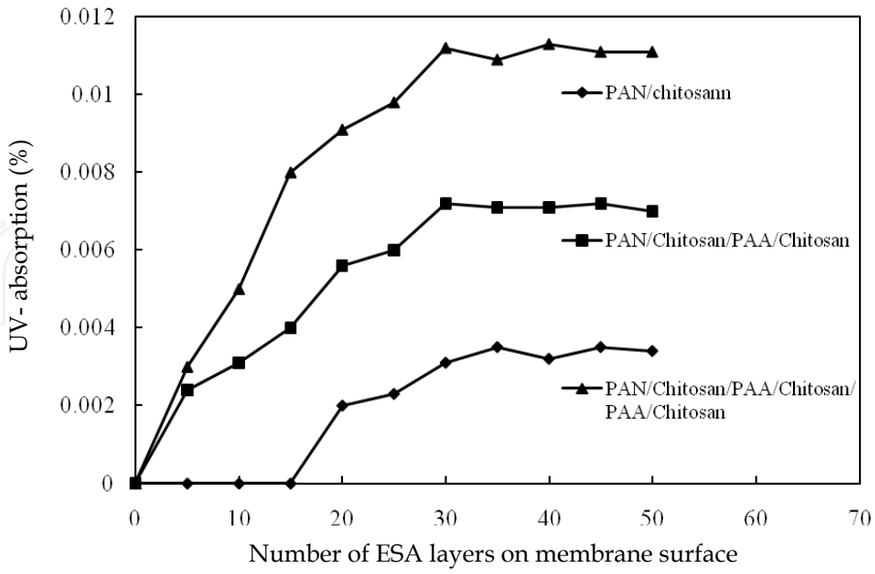

Fig. 4-3. The effect of immerging time on UV-absorption.

which verified the alternate self-assembly of chitosan (chitosan microsphere) layers and PAA layers onto charged substrate. When the substrate was immersed into chitosan microsphere, there was a remarkable increase in UV-absorption proving that a certain amount of chitosan had deposited onto substrate surface. Also, the samples immersed into the solutions of chitosan (chitosan microsphere) and PAA for 30 mins showed higher UV-absorption, which indicated the increase of the deposited amount of chitosan (chitosan microsphere).

Then, we examined the effect of immerging time on the self-assembly of chitosan for PAN/chitosan/PAA system.

It was thought from data that the self-assembly deposition of chitosan layer onto substrate surface reached saturated state after 30 mins. So, each deposited step lasted for 40 mins as to effectively reversed the charge on the membrane surface.

Characterization of ESA multilayer membranes by FT-IR

The surface of membranes having alternate ESA multilayer was investigated by using reflection FT-IR spectroscopy. Results are shown in Figure 4-4(a) and Figure 4-4(b) for PAN/chitosan/PAA system and PAN/chitosan microspheres/PAA system, respectively. It was found that the characteristic band of CN group from the charged PAN base membrane at about 2300 cm^{-1} became weaker due to the deposition of ESA layers of chitosan or chitosan microgel and PAA. In addition, the characteristic band at about 1170 cm^{-1} corresponding to the primary alcoholic group of chitosan. The peak at about 1400 cm^{-1} was assigned to the stretching vibration of amide band from chitosan appeared in the spectra, especially for cycled 1 and 3, for which the surface was terminated with chitosan layer or chitosan microspheres layer. In the cases of cycle 2 and 4 for surfaces terminated with PAA layer, similar spectra with PAA were observed and it was believed to be resulted by the

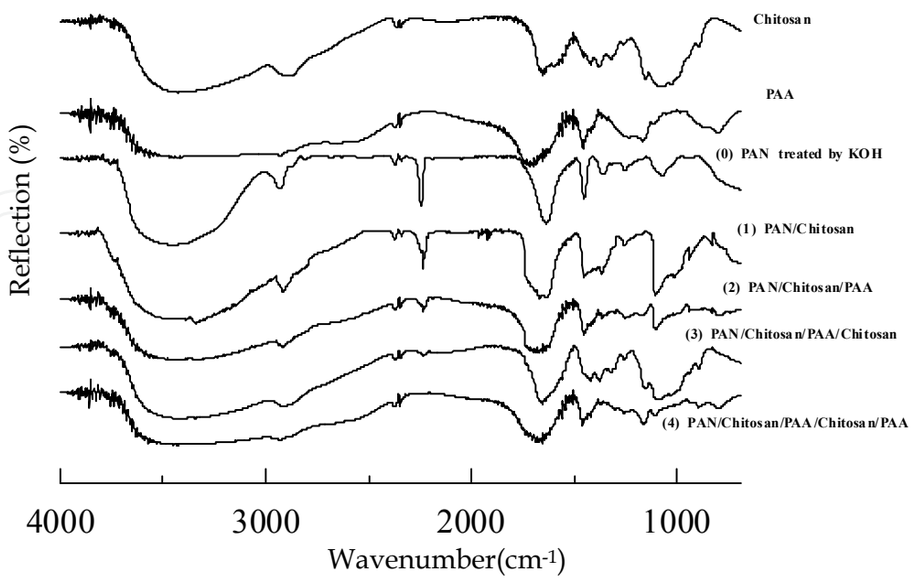

(a) PAN/Chitosan/PAA system

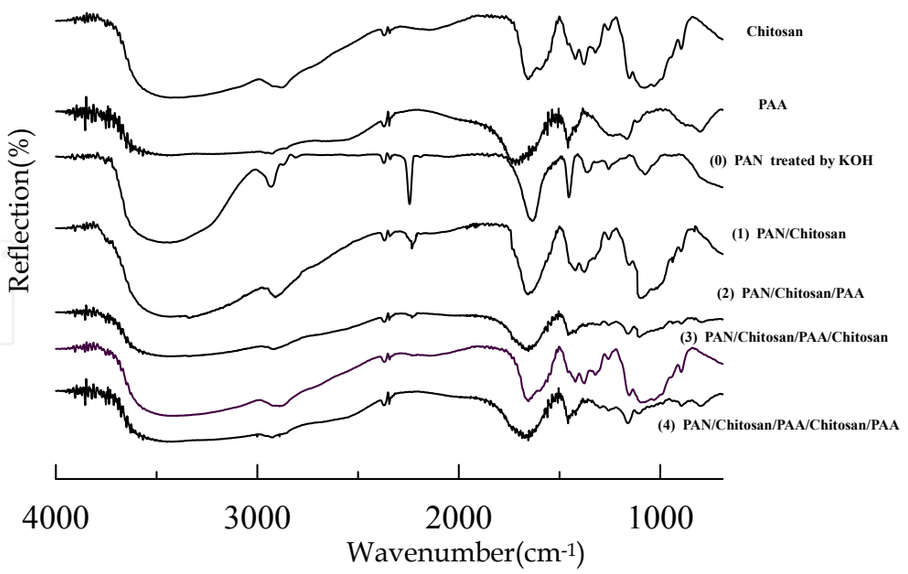

(b) PAN/Chitosan microsphere/PAA system

Fig. 4-4. FT-IR spectra of membranes with self-assembled layers.

coverage of PAA on membrane surface. It was also noted that the characteristic peak from chitosan became weaker, while the peak in the range of about 2500 cm^{-1} to 3750 cm^{-1} from the PAA layer became stronger, proving that the PAA layer converted the chitosan or chitosan microspheres layers on the surface. The upper change was repeated alternately along with the alternative deposition of chitosan (chitosan microspheres) layers and PAA layers onto charged PAN membrane as revealed by IR spectrum. These spectral changes proved the successful formation of alternate chitosan or chitosan microspheres layers and PAA layers onto charged PAN membrane surface. Furthermore, the obvious difference between the IR spectrum of PAN/Chitosan/PAA system and PAN/Chitosan microspheres/PAA system was observed in comparison of (a) and (b). For the PAN/Chitosan microsphers/PAA system, the disappearance of the peak of the CN group from the charged PAN base membrane was drastic due to the coverage of the ESA layers.

Surface roughness of the chitosan microspheres/PAA membranes were represented in Figure 4-5. As shown in Figure 4-5, the surface roughness of -1 and 0 which referred to membranes before and after NaOH treatment, indicated that the membrane surface became rougher due to the existence of hydrophilic carboxyl groups resulting from NaOH treatment. It was also apparent that the surface morphology was dramatically altered by the formation of the chitosan microspheres/PAA ESA multilayer. While the corresponding surface roughness values were 8.0 nm, 23.1 nm, 15.0 nm, 39.9 nm and 36.4 nm for the chitosan microspheres/PAA membranes with cycle layers of 0, 1, 2, 3 and 4, respectively.

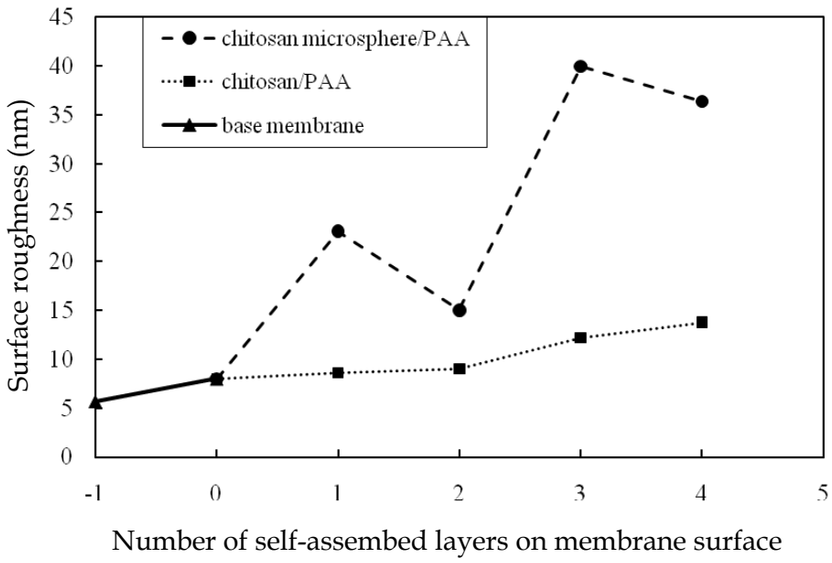

Fig. 4-5. Influence of numbers of self-assembled layers onto the membrane surface on the surface

However, much less change in the surface roughness was observed for the membrane with chitosan/PAA ESA layers. The values of the surface roughness were 8.0 nm, 8.6 nm, 9.0 nm, 12.2 nm, and 13.7 nm for the cycled layers of 0, 1, 2, 3 and 4, respectively. Therefore, the introduction of the chitosan microspheres for the ESA multilayer could be effectively for roughing the base of membrane surfaces. Therefore, this approach could be attractive in the uses of adsorption of such metal ions.

Adsorption capability for copper ion

It was known that chitosan could be applied for adsorption of metal ions since the amino group is capable of binding metal ions as served as coordination sites. For example, Juang et al.,[25] reported high selectivity for Cu^{2+} ion was observed by chitosan adsorbents. Chang et al[26] found that the chitosan-modified microsphere showed the largest equilibrium adsorption capacity at pH 5.5. Therefore, in the present work, we studied the binding capability for Cu^{2+} ion of the resultant membrane at various pHs.

Here, the pH of the Cu^{2+} ion solution was adjusted using buffer solution of 0.2 mol / L CH_3COOH and 0.2 mol / L CH_3COONa. The assembled behaviour of chitosan onto negatively charged base membrane and binding behaviour of chitosan for copper ions is simply illustrated by Scheme 4-4. Figure 4-6 shows the effect of the pH of Cu^{2+} ion solution on the Cu^{2+} adsorption of resultant membranes with Chitosan microspheres/PAA multiple-layers. The adsorption amounts of the Cu^{2+} ion were plotted at the cycle number for the ESA multilayer formation. The odd layers were for the chitosan or chitosan microspheres layers exposed on the membrane surface outmost and evens were for PAA layers on the outmost. It could be seen that when the adsorption was carried out at pH 3, membranes terminated with PAA layers showed higher adsorption capacity rather than those with terminal chitosan or chitosan microspheres layers. But, when pH increased, the change regulation could not be seen at pH 7 in both (a) and (b) systems. In the case of the chitosan microspheres/PAA system, the values of the adsorption capacity were significantly decreased to be in the range of about 50 ppm / g-membrane. However, at pH 5 and 6, the values of the adsorption capacity increased with the increasing of the cycled number of the

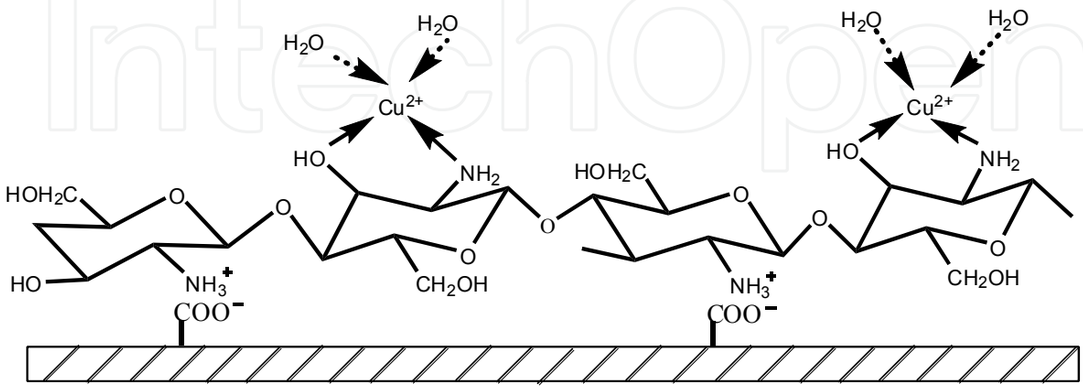

Scheme 4-4. Illustration images of the chelation for Cu^{2+} by the assembled chitosan on negatively charged membrane surface.

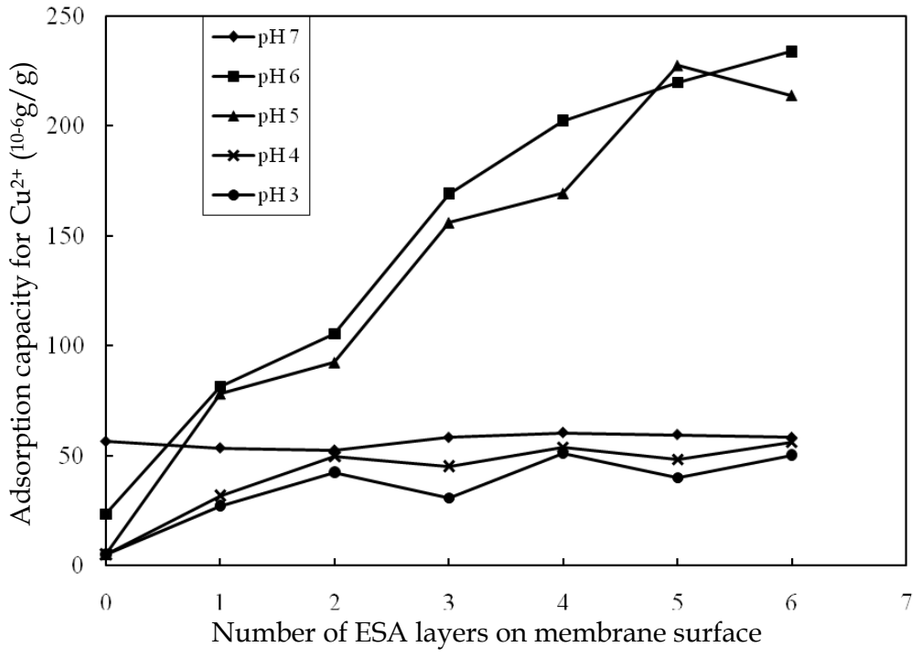

Fig. 4-6. Effect of the copper solution pH on the adsorption capacity of the resultant membranes of PAN/chitosan microsphere/PAA system.

ESA operation and then ranged in about 200-240 ppm / g-membrane. It was thought that the adsorption capacity of resultant membrane depended on the isoelectric point of chitosan, which was at about 6.3. At below the pH, the protonation of amine groups of chitosan could occur, while at higher pH the group behaved as non-protonated group. However, the binding ability of chitosan for copper ions was mainly due to the amine groups which were served as coordination sites for the sequestration of copper ion.[27] At lower pH, most of the amine groups in the chitosan segments was protonated and not available for copper uptaking by chelation. Thus, the values of the adsorption capacity decreased with decreasing pH. However, as the protonaed chitosan at low pH was able to bind anions by electrostatic attraction.[28] So, the resultant membranes showed a tendency with low adsorption capacity for Cu^{2+} ion at low pH region. But, at pH 7, the adsorption capacity became dramatically lower relative to roughness for the two systems. those at pH 5 and 6 for the chitosan microspheres/PAA system. It was considered that, at higher pH, the destruction of the self-assembled layers might have occurred, since the chitosan layers on membrane surface behaved as non-charged forms.

Especially the chitosan microspheres/PAA system demonstrated low adsorption at pH 7. This meant that the increase of the solution pH restrained the coordination of Cu^{2+} ions, which was induced by the destruction of the ESA multilayer at pH 7. However, at pH 5 and 6, partial amino group remained on the protonation form which was favorable for the stability of chitosan or chitosan microspheres layers on resultant membranes. Also, Figure 4-7 was plotted for comparing the adsorption capacity of resultant membranes with chitosan/PAA ESA layers and chitosan microspheres/PAA ESA layers. It was seen that

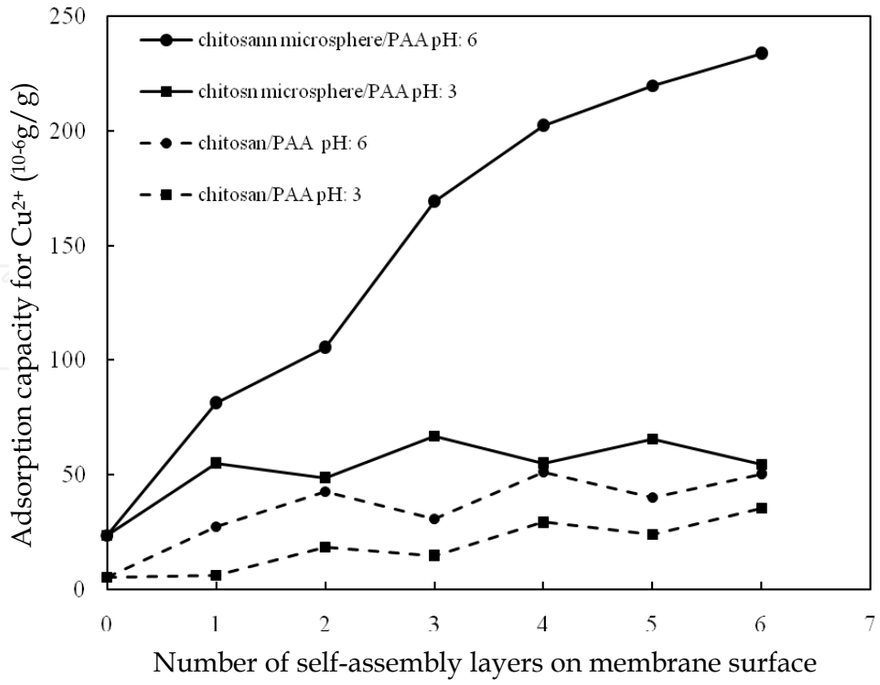

Fig. 4-7. Comparison of the adsorption capacity for Cu^{2+} of the two kinds of resultant membranes.

adsorption capacity of membranes functionalized with chitosan microspheres/PAA ESA layers at pH 6 was several times higher than that of membranes modified with chitosan/PAA ESA layers. The reason for this might be due to the fact that even though the crossing-linking of chitosan in the chitosan microsphere significantly reduced the chelating sites. There were still large amounts of residual amino and dydroxyl groups retained in the microsphere which were active for chelation. So, it was suggested that the ESA multilayer of chitosan microsphers/PAA onto charged substrate prepared in the present paper showed great potential in functioning membranes with high removal capability of heavy metal ions.

5. Conclusion

In the present chapter layer-by-layer electrostatic self-assembly technique was used for the preparation of functional polymeric membranes with metal ion removal capability. The fabrication process and properties of the resultant membranes were mentioned by using data of FT-IR spectra in detail.

A negatively charged P (AN-*co*-AA) membrane and positively charged P (AN-*co*-EDAMA) were used as the substrates for the ESA treatment. The desalination behaviour of the ESA multilayer modified resultant membranes was studied by evaluating the metal-ion removal properties for Fe^{3+} and Fe^{2+}. It was found that the resultant membrane showed higher rejection for trivalent ion than divalent metal ion. Evidences indicated that the alternate layer-by-layer formation of the ESA multilayer on the base membrane surface effectively influenced the metal-ion removal of the resultant membranes, indicating that ESA technique was useful for introducing the functionality.

Membranes with chelation capability were prepared by the alternate self-assembled of chitosan layer and PAA layer on PAN membrane surface. Taking advantage of the adequate surface area and a large amount of loading sites for metal ions, chitosan microspheres were synthesized and used as cationic species for the construction of ESA multilayer. The result of adsorption experimental for Cu(II) showed that the layer-by-layer deposition of chitosan/PAA or chitosan microspheres/PAA on charged base membrane surface was functionally equipped it with chelating ability for Cu^{2+}. Especially, because of the large internal porosities of the chitasan microspheres, resultant membranes with chitosan microspheres multilayer on the surface showed higher adsorption capacity for Cu^{2+} as compared with membranes modified by chitosan multilayer. This confirmed that fabrication of chitosan microsphere ESA multiplayer effectively improved the metal-ion uptake capability of membrane. It suggested that such membranes are expected to be applicable as a novel prospect for wastewater treatment.

6. Acknowledgment

We thank the supporting of Program for Project supported by forming a Hub for Human Resources Development and New Industry Creation Building a Sustainable Society Through Highly Interactive, Cooperative Educational Research with Pacific Rim Countries**.**

7. References

[1] Zapotoczny, S.; Golonka, M. & Nowakowska, M. (2005). Novel Photoactive Polymeric Multilayer Films. *Macromol. Rapid Commun,* Vol. 26, pp. 1049-1054.

[2] Kweon, D. K.; Song, S. B. & Park, Y. Y. (2003). Preparation of water-soluble chitosan/heparin complex and its application as wound healing accelerator. *Biomaterials*, Vol.24, pp. 1595-1601.

[3] Lojou, E. & Bianco, P. (2004). Buildup of Polyelectrolyte-Protein Multilayer Assemblies on Gold Electrodes. Role of the Hydrophobic Effect. *Langmuir*. Vol.20, pp. 748-755.

[4] Kozlovskaya, V.; Ok, S.; Sousa, S.; Libera, M. & Sukhishvili, S. A. (2003). Hydrogen-Bonded Polymer Capsules Formed by Layer-by-Layer Self-Assembly. *Macromolecules* Vol.36, pp. 8590-8592.

[5] Kim, Y. S.; Koo, J. Y. & Kim, H. (2008). Interplay of Hydrogen-Bond and Coordinate Covalent-Bond Interactions in Self-Assembly of NH_3 Molecules on the Si(001) Surface. *Phys. Rev. Lett,* Vol.100, pp. 256105-1-256105-4.

[6] Jiang, S. P.; Liu, Z. & Tian, Z. Q. (2006). Layer-by-Layer Self-Assembly of Composite Polyelectrolyte – Nafion Membranes for Direct Methanol Fuel Cells. *Adv. Mater.* Vol.18, pp. 1068-1072.

[7] Decher, G. (1997). Fuzzy Nanoassemblies: Toward Layered Polymeric Multicomposites. *Science.* Vol.277, pp. 1232-1237.

[8] Krasemann, L. & Tieke, B. Selective Ion Transport across Self-Assembled Alternating Multilayers of Cationic and Anionic Polyelectrolytes. *Langmuir*. Vol.16, pp. 287-290.

[9] Farhat, T. R. & Schlenoff, J. B.; (2003). Doping-Controlled Ion Diffusion in Polyelectrolyte Multilayers: Mass Transport in Reluctant Exchangers. *J. Am. Chem. Soc.* Vol.125, pp. 4627-4636.

[10] Li, J. Y.; Ichizuri, S.; Asanato, S.; Mutou, F.; Ikeda, S.; Iida, M.; Miura, T.; Oshima, A.; Tabata, Y. & Washio, M. (2006). Preparation of Ion Exchange Membranes by

Preirradiation Induced Grafting of Styrene/Divinylbenzene into Crosslinked PTFE Films and Successive Sulfonation. *J. Appl. Polym. Sci.* Vol.101, pp. 3587-3599.

[11] Cakmak, G.; Zorlu, F.; Severcan, M. & Severcan, F. (2011). Screening of Protective Effect of Amifostine on Radiation-Induced Structural and Functional Variations in Rat Liver Microsomal Membranes by FT-IR Spectroscopy. *Anal. Chem.* Vol.83, pp. 2438–2444.

[12] Arrondo, J. L. R.; & Goni, F. M. (1999). Structure and dynamics of membrane proteins as studied by infrared spectroscopy. *Progress in Biophysics & Molecular Biology.* Vol.72, pp. 367-405.

[13] Li, J.; Wong, M. W.; Lin, L.; Bianchi, V.; Edwards, M. & Yip, C. M. (2011) IR Spectroscopy of Protein and Peptide-Membrane Interactions. *Biophys. J.* Vol.100, pp. 495a.

[14] Sukumaran, S.; Hauser, K.; Rauscher, A. & Mantele, W. (2005) Thermal stability of outer membrane protein porin from *Paracoccus denitrificans*: FT-IR as a spectroscopic tool to study lipid–protein interaction. *FEBS Letters.* Vol.579, pp. 2546-2550.

[15] Luo, M. L.; Wen, Q. Z.; Liu, J. L.; Liu, H. J. & Jia, Z. (2011) Fabrication of SPES/Nano-TiO2 Composite Ultrafiltration Membrane and Its Anti-fouling Mechanism. *Chin. J. Chem. Eng*. Vol.19, pp 45-51.

[16] Xua, H. K.; Fanga, J.; Guo, M.; Lua, X. H.; Wei, X. L. & Tu, S. (2010) Novel anion exchange membrane based on copolymer of methyl methacrylate, vinylbenzyl chloride and ethyl acrylate for alkaline fuel cells. *Journal of Membrane Science.* Vol.354, pp 206-211.

[17] Tang, B. B.; Wu, P. Y. & Siesler, H. W. (2008). In Situ Study of Diffusion and Interaction of Water and Mono- or Divalent Anions in a Positively Charged Membrane Using Two-Dimensional Correlation FT-IR/Attenuated Total Reflection Spectroscopy. *J. Phys. Chem. B*. Vol.112, pp. 2880–2887.

[18] Ding, Y.; Bikson, B. & Nelson, J. K. (2002). Polyimide Membranes Derived from Poly(amic acid) Salt Precursor Polymers. 2. Composite Membrane Preparation. *Macromolecules* Vol.35, pp. 912–916.

[19] Kobayashi, T.; Fu, H. T.; Cui, Q. & Wang, H. Y. (2008). Multilayer Composite Surfaces Prepared by an Electrostatic Self-Assembly Technique with Quaternary Ammonium Salt and Poly(acrylic acid) on Poly(acrylonitrile-co-acrylic acid) Membranes. *J. Appl. Polym. Sci.* Vol.110, pp. 3234-3241.

[20] Kobayashi, T.; Kumagai, K.; Nosaka, Y.; Miyama, H.; Fujii, N. & Tanzawa, H. (1991). Permeation behavior of dextrans by charged ultrafiltration membranes of polyacrylonitrile photografted with ionic monomers. *J. Appl. Polym. Sci.* Vol.43, pp. 1037-1043.

[21] Arica, M. Y.; Yilmaz, M. & Bayramoglu, G. (2007). Chitosan-grafted poly(hydroxyethyl methacrylate-co-glycidyl methacrylate) membranes for reversible enzyme immobilization. *J. Appl. Polym. Sci.* Vol.103, pp. 3084-3093.

[22] Wang, D. X.; Su, M.; Yu, Z. Y.; Wang, X. L.; Ando, M. & Shintani, T. (2005). Separation performance of a nanofiltration membrane influenced by species and concentration of ions. *Desalination.* Vol.175, pp. 219-225.

[23] Wang, X. L.; Tsuru, T.; Nakao, S. & Kimura, S. (1997). The electrostatic and steric-hindrance model for the transport of charged solutes through nanofiltration membranes. *J. Membr. Sci.* Vol.135, pp. 19-32.

[24] Kobayashi, T.; Wang, H. Y. & Fujii, N. (1998). Molecular imprint membranes of polyacrylonitrile copolymers with different acrylic acid segments. *Anal. Chim. Acta.* Vol.365, pp. 81-88.

[25] Jang, R. S. & Shao, H. J. (2002). Effect of pH on Competitive Adsorption of Cu(II), Ni(II), and Zn(II) from Water onto Chitosan Beads. *Adsorption.* Vol.8, pp. 71-78.

[26] Chang, Y. C.; Chang, S. W. & Chen, D. H. (2006). Magnetic chitosan nanoparticles: Studies on chitosan binding and adsorption of Co(II) ions. *Reac. Func. Polym.* Vol.66, pp. 335-341.

[27] Dambies, L.; Guimon, C.; Yiacoumi, S. & Guibai. E. (2000). Characterization of metal ion interactions with chitosan by X-ray photoelectron spectroscopy. *Colloids Surf. A*. Vol.77, pp. 203-214.

[28] Guibal, E. (2004). Interactions of metal ions with chitosan-based sorbents: a review. *Separation and Purification Technology*. Vol.38, pp. 43-74.

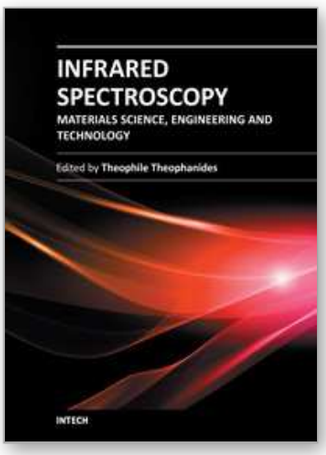

Infrared Spectroscopy - Materials Science, Engineering and Technology

Edited by Prof. Theophanides Theophile

ISBN 978-953-51-0537-4
Hard cover, 510 pages
Publisher InTech
Published online 25, April, 2012
Published in print edition April, 2012

The present book is a definitive review in the field of Infrared (IR) and Near Infrared (NIR) Spectroscopies, which are powerful, non invasive imaging techniques. This book brings together multidisciplinary chapters written by leading authorities in the area. The book provides a thorough overview of progress in the field of applications of IR and NIR spectroscopy in Materials Science, Engineering and Technology. Through a presentation of diverse applications, this book aims at bridging various disciplines and provides a platform for collaborations among scientists.

How to reference

In order to correctly reference this scholarly work, feel free to copy and paste the following:

Weimin Zhou, Huitan Fu and Takaomi Kobayashi (2012). Infrared Analysis of Electrostatic Layer-By-Layer Polymer Membranes Having Characteristics of Heavy Metal Ion Desalination, Infrared Spectroscopy - Materials Science, Engineering and Technology, Prof. Theophanides Theophile (Ed.), ISBN: 978-953-51-0537-4, InTech, Available from: http://www.intechopen.com/books/infrared-spectroscopy-materials-science-engineering-and-technology/infrared-analysis-of-electrostatic-layer-by-layer-polymer-membranes-having-characteristics-of-heavy

INTECH
open science | open minds

InTech Europe
University Campus STeP Ri
Slavka Krautzeka 83/A
51000 Rijeka, Croatia
Phone: +385 (51) 770 447
Fax: +385 (51) 686 166
www.intechopen.com

InTech China
Unit 405, Office Block, Hotel Equatorial Shanghai
No.65, Yan An Road (West), Shanghai, 200040, China
中国上海市延安西路65号上海国际贵都大饭店办公楼405单元
Phone: +86-21-62489820
Fax: +86-21-62489821

IntechOpen